

## SPH SIMULATIONS OF A LOBE PUMP: PREDICTION OF PROTEIN SHEAR STRESS AT DIFFERENT PUMP EFFICIENCIES

Mahesh PRAKASH<sup>1</sup>, Nick STOKES<sup>1</sup>  
Joseph BERTOLINI<sup>2</sup>, Owen TATFORD<sup>2</sup>, Peter GOMME<sup>2</sup>

<sup>1</sup>CSIRO Mathematical and Information Sciences, Clayton, Victoria 3169, AUSTRALIA

<sup>2</sup>CSL Bioplasma, Broadmeadows, Victoria 3047, AUSTRALIA

### ABSTRACT

Using Smoothed Particle Hydrodynamics (SPH), the motion of a Lobe Pump under load was simulated in order to predict variations in shear stress and pump efficiency with varying gap size (1, 2, 4 mm) between the lobes and pump housing. The simulations indicated that pump shear was dependent on gap size, with shear stress levels (0 – 40 Pa) correlating to those obtained from Couette rheo-optic experiments (0 – 30 Pa). As gap size increased the number of fluid particles experiencing low shear (< 10 Pa) increased only fractionally whereas those experiencing high shear (>20 Pa) showed a decreasing trend. The pump efficiency however decreased considerably with gap size, requiring more lobe revolutions to pass a unit volume. Taken together these observations indicate that pumps operated with increased gaps between the lobe and housing result in larger number of particles within the fluid experiencing shear stresses. Moreover, the simulations indicate that it is best to use larger lobe pumps operated at high efficiency to transfer protein containing solutions.

### INTRODUCTION

Lobe pumps are often used to transfer fluids containing protein. Using a lobe pump can impart high shear stress leading to protein instability. This can be aggravated by wear and tear on the pump, as the gap between the lobes and the pump housing increases. This reduces the efficiency of the pump, leading to higher rotation rates, which increase shear related damage to the protein.

Smoothed Particle Hydrodynamics (SPH) is a Lagrangian method for modelling fluid flows and heat transfer. Materials are approximated by particles that are free to move around rather than by fixed grids or meshes. For further information about SPH refer to Gingold and Monaghan (1977), Monaghan (1994), Cleary (1998) and Cleary et al (2002).

SPH is particularly well suited to momentum dominated flows, flows involving complex free surface behaviour and flows involving complex physics such as solidification or flow through industrial porous media. It is also useful for flows around moving objects, since there are no mesh structures to be affected. Due to these advantages, simulations of a Lobe Pump were carried out using SPH to determine regions of high shear stress and to explore the possibility of obtaining pump efficiencies at different gap sizes between the pump housing and the lobes.

This paper details the results that were obtained for 2D simulations at moderate resolution. They represent a Waukesha (Universal Series) pump. As shown in Figure 1 the lobe pump used for the present simulation consists of two rotors moving inside the pump housing. A 2d cross-section of the lobe pump shown below was used to represent the motion of the fluid and the rotors in a real situation (see Figure 2)

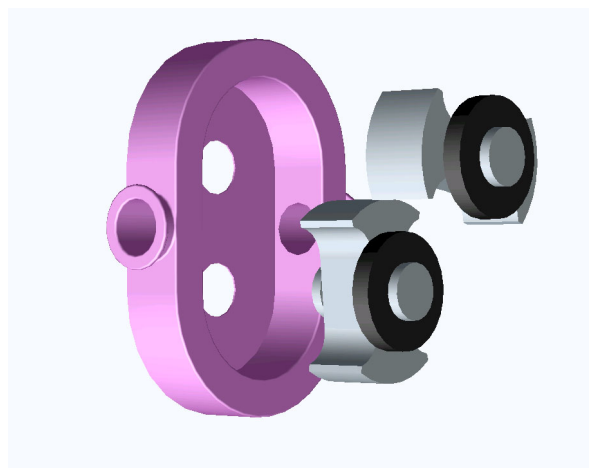


Figure 1: 3D view of pump housing and rotors of a lobe pump

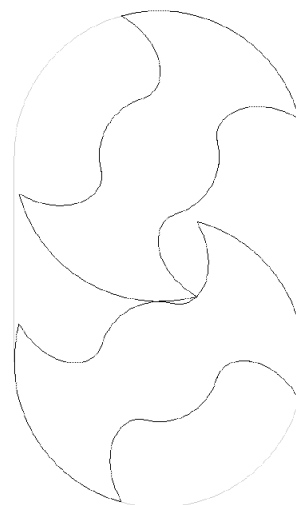
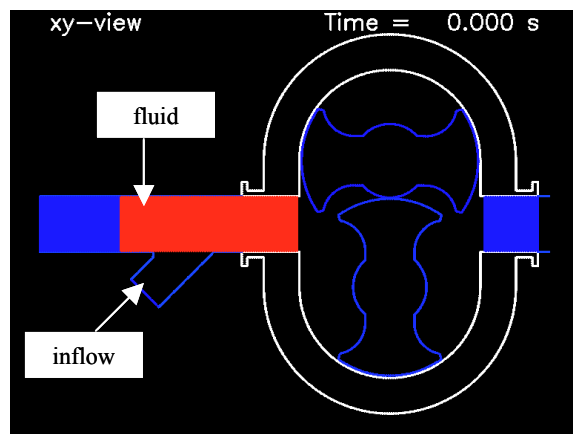


Figure 2: 2D cross-section of the lobe pump used for SPH simulations

## MODEL DESCRIPTION

### Setting up the simulation

The 2D geometry was set-up by using an in-house particle pre-processor. Figure 3 shows the 2D configuration. The pump chamber initially does not contain any fluid. The discharge pipe on the right is connected to the inlet pipe using a periodic boundary condition. Fluid is filled into the system using an inflow boundary condition in a side pipe attached to the main inlet pipe of the pump as indicated in the figure. The inlet and outlet pipes are initially filled with fluid. Part of the fluid (fluid coloured red in Figure 3) has an initial velocity of 1.5 m/s matching the inlet fluid velocity. The fluid coloured blue in the figure has a zero initial velocity.



**Figure 3:** 2D lobe pump set-up using in-house particle pre-processor.

A load is applied to the above system by applying a resistance in a region upstream of the pump in the form of a porous plug of appropriate permeability (using Darcy's law) as shown in Figure 4. The inflow used was an applied pressure inflow with a pressure of 50 kPa and a maximum inflow velocity of 1.5 m/s. The inflow automatically cuts off once the pump is full and the system pressurises to the specified pressure. The rotor speed was set to a value of 170 rpm. The pressure drop across the system was monitored by using a set of pressure sensors shown in Figure 4. Sensor 1 located on the rotor is used to represent the motion of the rotors. Sensors 2, 3 and 4 are used to monitor the pressure close to the inlet of the pump. Sensors 5, 6 and 7 are used to monitor the pressure close to the outlet of the pump and Sensor 8 records the pressure close to the inflow. The pressure drop across the pump is the difference in the sensor readings recorded at the outlet and the inlet of the pump.

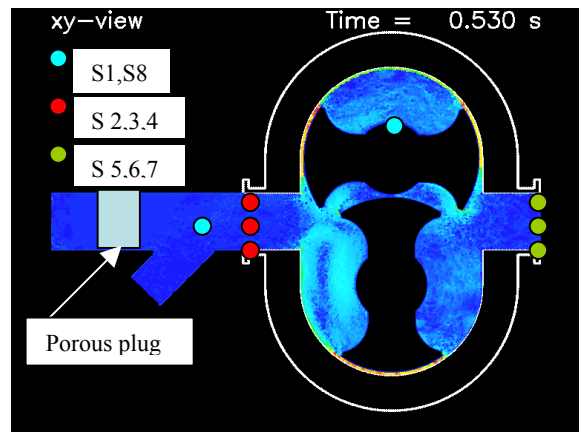


**Figure 4:** Location of pressure sensors and porous plug. (S1 used for rotor movement).

Three different simulations were run with a gap width of 1.0, 2.0 and 4.0 mm between the rotor and pump housing. The particle size of the SPH particles for all three simulations was 1.0 mm. This means that with a gap width of 1.0 mm the fluid is just able to go through the gap between the rotor and pump housing. This case was considered to be close to a maximum efficiency pump. With a gap of 2.0 and 4.0 mm, the fluid is more easily able to pass between the rotor and pump housing. There will also be an increase in the backflow at the centre where the two rotors meet each other with an increase in the gap width. This means that there will be a decrease in the pump efficiency with an increase in gap width. The efficiency has been calculated on the basis of average x-momentum across the pump. A decrease in efficiency means a drop in the average x-momentum. For all three simulations reported here, the permeability of the porous plug was fixed at  $K = 4 \times 10^{-10} \text{ m}^2$ . Using Darcy's law this gives a pressure drop across the pump of about 200 kPa for close to an ideal pump (gap = 1.0 mm). With an increase in the gap width, there will be a decrease in the pressure drop across the pump indicating a drop in efficiency.

In order to assess the possibility of rupture of protein cells a shear stress analysis was carried out for all three simulations. Particles undergoing shear were graded as per the amount of shear they experience. Particles experiencing high shear stress were classified as possible candidates to undergo protein rupture. As reported in the section below an order of magnitude comparison was carried out with Couette chamber experiments (Johnston, 2002) to estimate a possible range of shear stress at which protein cells start getting damaged.

## RESULTS AND DISCUSSION

### Filling of the Pump and Velocity Distribution

Figure 5 shows various stages of the filling process of the pump, coloured by the magnitude of velocity for a gap width of 1.0 mm. The pump is almost fully filled in about 0.4 seconds. Once the filling is completed the inflow stops generating fluid particles. The fluid in the chamber now moves only due to the movement of the rotors. As shown in Figure 5d above, once the filling is complete, there is a high velocity region close to the gap between the pump-

housing and the rotors as the fluid tries to rush into this area.

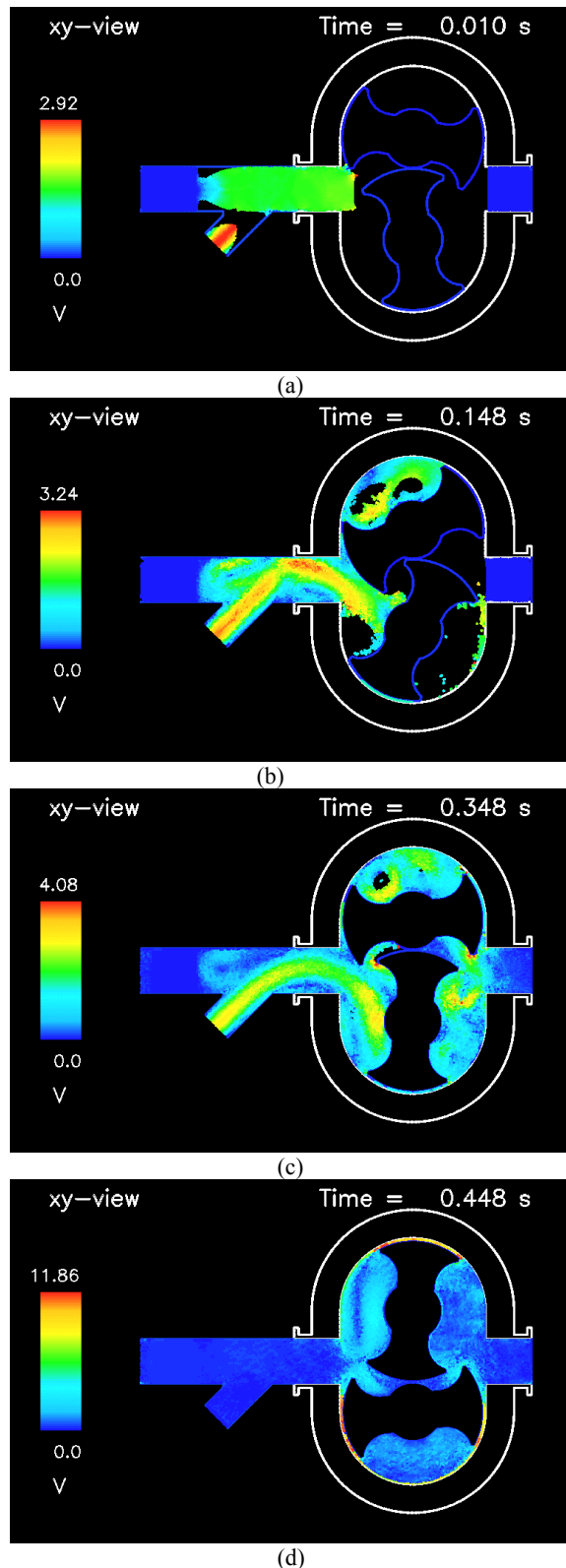


**Figure 5:** Filling of the pump and subsequent steady rotor motion at a gap width of 1.0 mm. The fluid is coloured by magnitude of the velocity.

The magnitude of the maximum velocity in these gaps decreases with an increase in the gap width as it becomes easier for the fluid to pass through the gap, see Figure 6. It

can also be seen from Figure 6 that with a gap of 1.0 mm no fluid can pass through the opening between the two rotors when the circular region at the centre of the rotor meets the outer semi-circular rotor blade. With an increase in the gap width, however, this opening is enough to generate a back-flow through this region (see frames b and c in Figure 6) resulting in a decrease in pump efficiency.

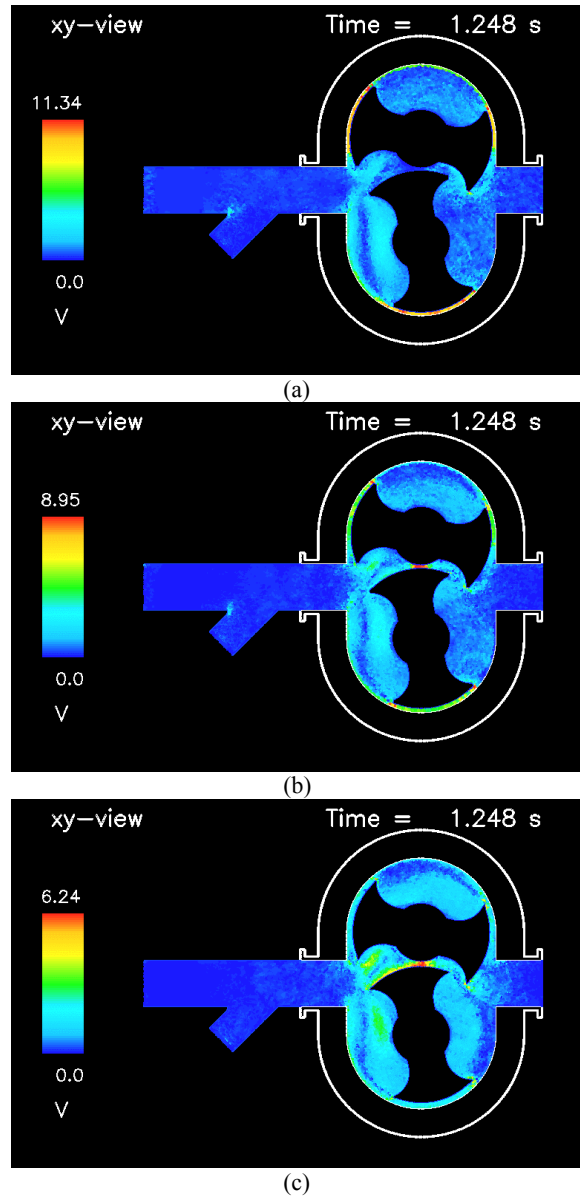


**Figure 6:** Simulations showing magnitude of velocity at gap widths of (a) 1.0 mm, (b) 2.0 mm and (c) 4.0 mm. Note that with an increase in the gap width there is a decrease in the maximum velocity in the gaps. Also, there is a high velocity region between the two rotors for gaps = 2.0 (b) and 4.0 (c) mm.

#### Shear Stress Distribution

Regions of high shear in the pump correspond to regions of high velocity differential. This is seen from Figure 7 which gives a comparison between shear stresses for each of the three cases at 1.248 seconds. One can also clearly see a drop in maximum shear stress values with an increase in the gap width. This is consistent with expectations since with an increase in gap width the velocity gradient should reduce. However, what is not

intuitive is the number of particles that undergo shear that is high enough to cause damage.

$$Shear = \mu \frac{(v_{max} - v_{min})}{\Delta x} \quad \text{eq 1}$$

where  $\mu$  is the fluid viscosity = 0.001 Pa s,  $v_{max}$  = velocity of the moving surface,  $v_{min}$  = minimum velocity = velocity at the wall = 0 m/s and  $\Delta x$  = gap in the Couette chamber =  $0.5 \times 10^{-3}$  m. The radius of the inner chamber is  $4.5 \times 10^{-3}$  m. At 183 rev/s  $v_{max} = 5.17$  m/s.

With the above maximum velocities the shear from Eq. 1 is calculated to be 10.3 Pa at a rotational speed of 183 rev/s. This means that one needs to have a shear force of about 10 Pa for the cells to be damaged.

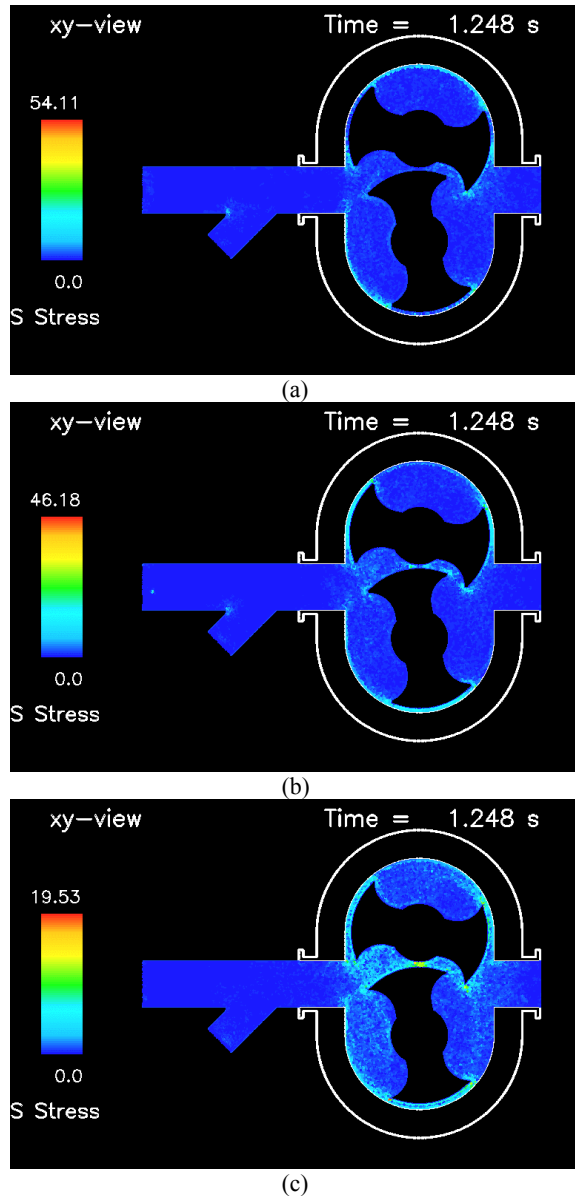


**Figure 7:** High shear stress regions in the pump correspond to regions of high velocity differential.

A better understanding of the variation in shear stress with gap comes from Figure 8 and Table 1 which give a breakdown of particles experiencing each range of shear stress values. Note that the values in Table 1 represent shear stress numbers for the three pumps run for the same amount of time or the same number of rotor revolutions. Experimental shear studies carried out using a Couette rheo-optic device (CSL Bioplasma, unpublished data) indicates that protein damage (in the form of an increase in turbidity level of the protein solution) occurs at a rotational speed of about 183 rev/s or a shear rate of 10 Pa. If one assumes that only the gradient of the velocity determines the shear force, the following equation gives the shear force:

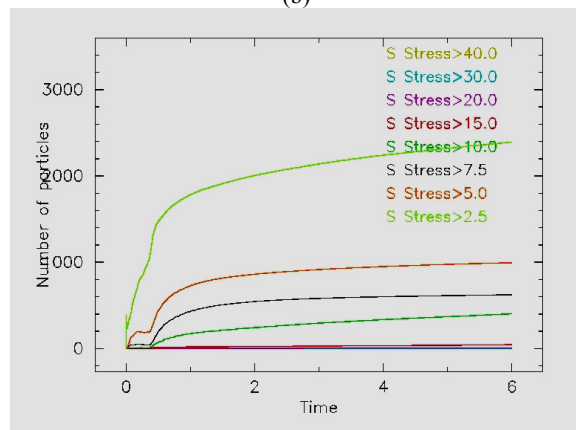
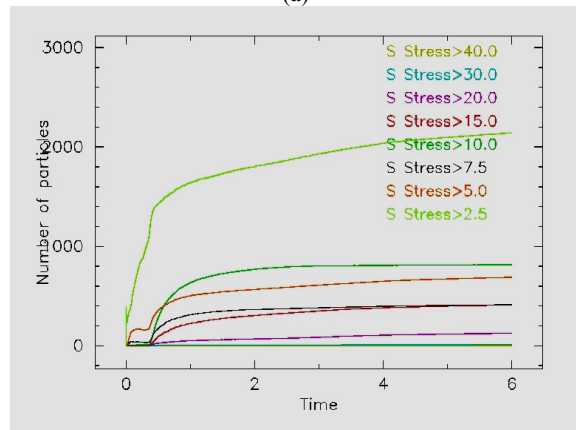
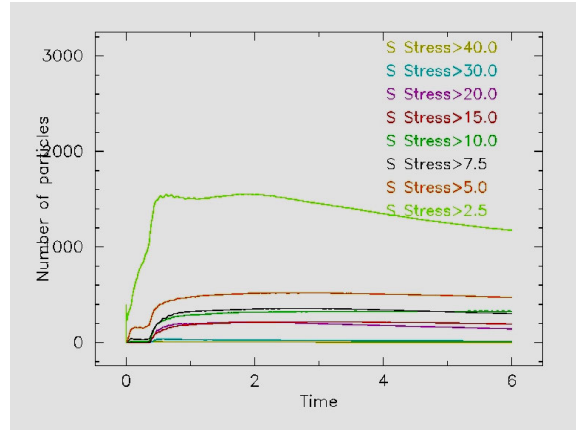


**Figure 8:** Shear stress distribution showing SPH particles experiencing a range of shear stress values for gaps of (a) 1.0 mm, (b) 2.0 mm and (c) 4.0 mm.

Gap mm	>2.5 Pa	>5.0 Pa	>7.5 Pa	>10 Pa	>15 Pa	>20 Pa	>30 Pa	>40 Pa
1.0	2631	1456	985	682	355	161	18	3
2.0	4609	2468	1779	1366	551	140	14	2
4.0	4467	2072	1079	456	54	9	0	0

**Table 1:** Average number of particles experiencing a cumulative range of shear stress for several cycles of the rotor. Pumps with different gap size are considered and are run for the same amount of time..

The shear stress range experienced by the fluid particles in the simulation (of the order of 10 to 40 Pa) correlates well with that found from the experiments. This gives some confidence in deducing conclusions from observations made in the simulations.

#### Efficiency of the Pump, Pressure drop and Shear Stress Based on Pump Efficiency

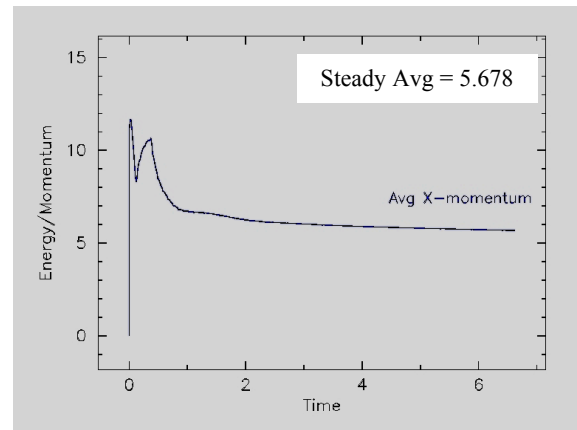
The average x-momentum for the three gap widths are plotted against time in Figure 9. From the plots it is clear that the simulations reach a steady state within about 2 seconds. The steady average values of the x-momentum for the gaps of 1.0, 2.0 and 4.0 mm are respectively, 5.678, 2.420 and 1.361 kg m/s. This means that the efficiency drops to about 43 % in going from 1.0 to 2.0 mm and to about 24 % in going from 1.0 to 4.0 mm.

Another indicator of drop in efficiency is a reduction in the pressure drop across the pump with an increase in gap size. Figure 10 shows pressure drop across the pump for the three gap sizes. For the purpose of clarity the readings from sensor 1 (representing the motion of the rotors), sensor 2 (close to the inlet of the pump) and sensor 5 (close to the outlet of the pump) are only shown in the figure.

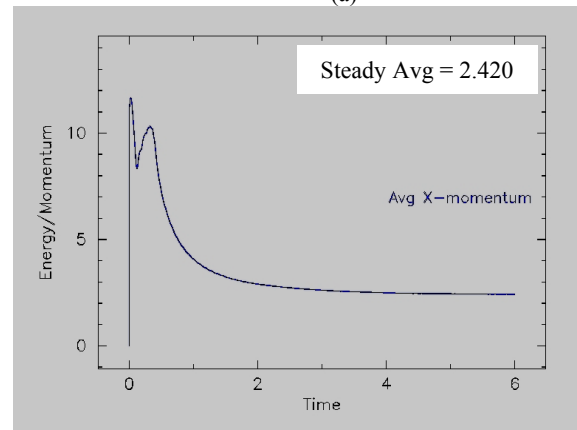
Refer to Figure 4 above to locate the position of pressure sensors 1 to 8. As expected sensors 2, 3, 4 (close to the inlet of the pump) and 8 (close to the inflow) recorded similar pressures once at steady state. Sensors 5, 6 and 7 (close to the outlet of the pump) recorded similar pressures as well.

The pressure drop is the difference in the pressure readings between these two values. With a gap of 1.0 mm the average pressure drop is about 180 kPa (frame a, Figure 10). Note that this pressure drop is reasonably close to the expected pressure drop of 200 kPa that was calculated using Darcy's law for a pump without any gap. With a gap of 2.0 mm (frame b, Figure 10) the pressure drop decreases to about 70 kPa. This is a decrease in pressure drop to about 39 % of the value at 1.0 mm. In going to a gap of 4.0 mm (frame c, Figure 10) the magnitude of pressure fluctuations are close to the magnitude of the pressure drop. Since the pressure fluctuates by about 30 kPa one can assume that this is approximately the magnitude of pressure drop at a gap of 4.0 mm. This give a decrease in pressure drop to about 16.7 % of the value at 1.0 mm. The drop in efficiency

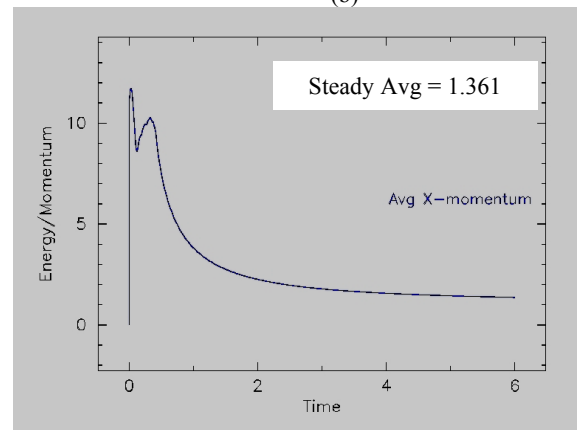
calculated from the pressure sensor readings thus correlate well with the drop in efficiency calculated from the reduction in average x-momentum at different gap sizes.



(a)



(b)



(c)

**Figure 9:** Average x-momentum for gap widths of (a) 1.0 mm, (b) 2.0 mm and (c) 4.0 mm

For a better understanding of the relationship between shear stress and gap width, the shear stress readings in Table 1 were normalised based on the pump efficiency with the same amount of fluid being passed for each of the three cases. These numbers are given in Table 2. Note that from Table 1 as the gap size increases the number of particles experiencing low shear (< 10 Pa) increases only fractionally whereas particles experiencing high shear (> 20 Pa) show a decreasing trend. In fact, the cumulative number of particles experiencing any reasonable amount

of shear (first column in Table 1) actually starts decreasing slightly at a gap width of 4.0mm. However, due to a reduction in the pump efficiency one requires more lobe revolutions to pass the same amount of fluid at a larger gap width. Due to this the number of particles experiencing shear shows a clear increasing trend with increase in gap width in Table 2 (see the first column). This indicates that pumps operated with increased gaps between the lobe and housing result in larger amounts of protein cells within the fluid experiencing non-negligible shear stresses.

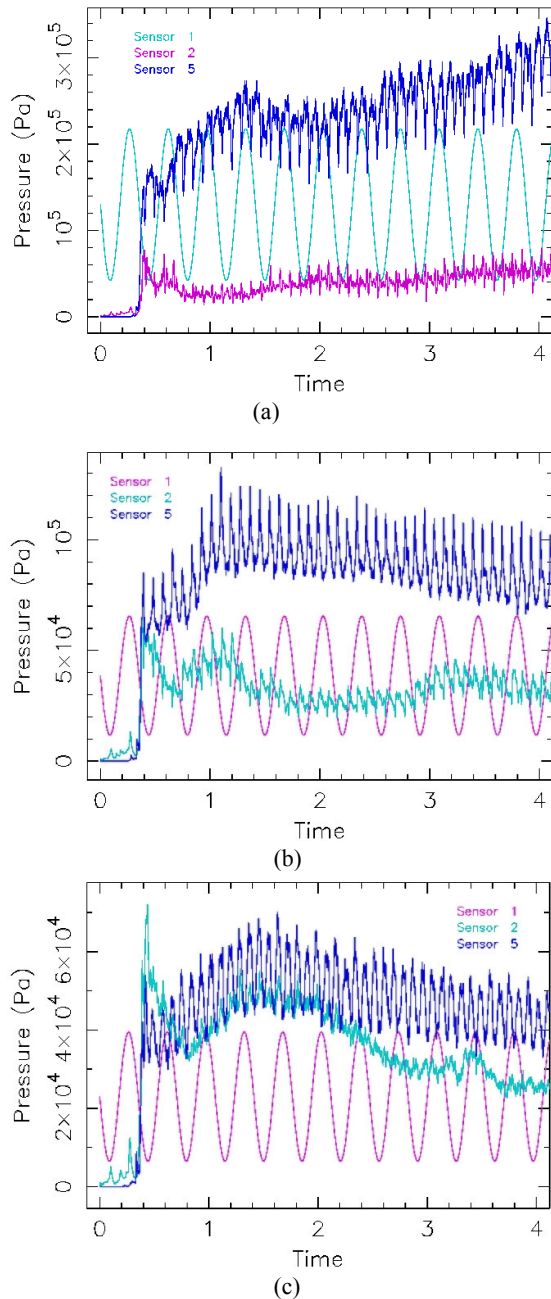


**Figure 10:** Pressure drop across the pump for gap widths of (a) 1.0 mm, (b) 2.0 mm and (c) 4.0 mm

Gap mm	>2.5 Pa	>5.0 Pa	>7.5 Pa	>10 Pa	>15 Pa	>20 Pa	>30 Pa	>40 Pa
1.0	2631	1456	985	682	355	161	18	3
2.0	10722	5742	4139	3178	1282	326	33	5
4.0	18615	8635	4497	1905	226	38	0	0

**Table 2:** The table compares the number of particles experiencing a cumulative range of shear stress with the same amount of fluid being passed through the pump at different gap sizes.

## CONCLUSIONS

Pump simulations were carried out with rotor to pump housing gaps of 1.0, 2.0 and 4.0 mm. With an increase in the gap width, the pump efficiency drops dramatically. For example, the efficiency drops to about 43% for the 2.0 mm gap and as low as 24% for the 4.0 mm gap in comparison with the 1.0 mm gap case. The drop in the efficiency was calculated on the basis of a drop in the average x momentum of the fluid. The increase in gap size also dramatically reduces the pressure drop across the pump. The shear stress range experienced by the fluid in the simulations and in the Couette rheo-optic experiments showed a similar order of magnitude giving confidence in the shear stress results obtained from the simulations. With an increase in gap width the number of particles experiencing any reasonable amount of shear starts to increase only slightly. However, due to a reduction in the pump efficiency one requires more lobe revolutions to pass the same amount of fluid at a larger gap width. Taken together these observations indicate that pumps operated with increased gaps between the lobe and housing result in larger number of particles within the fluid experiencing non-negligible shear stresses.

## ACKNOWLEDGMENTS

The authors would like to thank Dr Paul Cleary for his valuable advice and suggestions during the course of this project

## REFERENCES

- CLEARY, P.W. (1998). Modelling confined multi-material heat and mass flows using SPH. *Applied Mathematical Modelling*, **22**, 981–993.
- CLEARY, P., HA, J., ALGUINE, V., NGUYEN, T., (2002), “Flow Modelling in Casting Processes”, *Applied Mathematical Modelling*, **26**, 171-190.
- GINGOLD, R.A. & MONAGHAN, J.J., (1977), Smoothed particle hydrodynamics. Theory and application to non-spherical stars., *Mon. Not. Roy. Astron. Soc.*, **181**, 375-389.
- MONAGHAN, J.J., (1994), “Simulating free surface flows with SPH”, *J. Comp. Phys.*, **110**, 399-406.